Control Hardware-in-the-Loop Demonstration of a Building-Scale DC Microgrid Utilizing Distributed Control Algorithm

Maziar Mobarrez
US Corporate Research Center
ABB
Raleigh, USA
maziar.mobarrez@us.abb.com

Niloofar Ghanbari and S. Bhattacharya
Department of Electrical and Computer Engineering
North Carolina State University
Raleigh, USA
nghanba@ncsu.edu

Abstract—**DC microgrids and DC distribution power systems offer efficiency improvement, higher reliability, better expandability and stability over their equivalent AC systems. Despite the clear advantages of DC distribution systems, the deployment of such systems does not make economical sense due to high engineering, installation and commissioning costs. In this paper, we are proposing a platform that is designed to enable DC microgrids by simplifying project-specific design, installation, and commissioning, allowing designers to unlock the benefits of microgrids for the customers in an economic manner. The proposed platform, utilizes a distributed control algorithm and the concept of multiple slack sources (for power sharing). This core structure enables microgrid advantages of redundancy, simple plug-and-play, modularity and expandability. In this paper, the proposed control structure is explained in details. Then, analytical analysis is performed to ensure the stability of the system in all the operating modes. Finally, Control Hardware-in-the-Loop (C-HIL) simulations are used for demonstrating the effectiveness and feasibility of the proposed platform in a typical photovoltaic (PV) plus battery energy storage (BESS) grid-interactive DC microgrid.**

Index Terms—**DC microgrid, Distributed Control, Power Sharing, Droop Control, Stability, Hardware-in-the-Loop, HIL, Real-Time Simulations.**

I. INTRODUCTION

While remarkable progress has been made in improving the performance of AC microgrids, DC microgrids have also been recognized as an attractive technology for many applications because of their higher efficiency, higher reliability, better expandability, improved stability, more natural interface to many types of renewable energy sources and ESSs, and better compliance with consumer electronics [1] - [5].

One of the challenges associated with employing DC microgrids, is to implement a reliable control algorithm that ensures all the power converters maintain stable power balance between generation and consumption [6] - [7]. While ensuring power balance, the control algorithm should also control power sharing among sources and allow for multiple slack sources for redundancy. Moreover, the control algorithm has to be distributed and enable system expansion with minimal engineering effort. Finally, the controller should be able to reliably mitigate the impact of PV and load variations in the microgrid from transferring to the AC power grid, when the microgrid is operating in grid-tied mode [2], [8]. Authors of this paper addressed the latter requirement in [1]. The focus of this paper is on the other mentioned requirements.

The basis of the proposed control platform is to achieve stability by paralleling voltage sources on the DC bus. Each source is able to regulate the voltage at its output and is designed with the knowledge of its topology, switches, power source, and output capacitance such that it is stable under any external load fluctuations within the limits of its power rating. In other words, each source is a "slack" terminal, similar to slack generators in power systems, in that it provides whatever power is necessary to ensure power balance and maintain the bus voltage. As a system expands to include multiple sources, the system is stable as long as each source is stable. This core structure enables microgrid advantages of redundancy, simple plug-and-play, modularity and expandability.

The first section of this paper, explains the control strategy in details as well as the design criteria of the different converters of the system. Next, analytical stability analysis is performed to ensure the stability of the system in all the operating modes. Finally, C-HIL simulations are used for demonstrating the effectiveness and feasibility of the proposed platform and control algorithm in a typical PV plus BESS grid-interactive DC microgrid.

II. CONTROL ALGORITHM

The basis of the proposed control platform is to achieve stability by paralleling voltage sources on the DC bus. The challenge that comes in paralleling voltage sources, is to control the amount of power each source contributes or absorbs. Without an additional control layer, sources may disproportionally source or sink power due to proximity and line impedances. Additionally, circulating currents can arise from slight differences in voltage feedback measurements, which is significant in microgrid systems with relatively small line impedances [6]. To control and balance the power contribution among sources, a virtual resistance is added in

the controller to dominate the effects of actual line resistance and feedback error. With multiple devices paralleled, their power contribution is proportional to their virtual resistances, allowing the system to achieve power sharing or alternatively prioritization of the sources. The virtual resistance control method is extended to defining a steady state voltage vs current function for each converter, such that the operating power of each device is defined at the specific global voltage. This control falls under the category of droop control, a well-established method of distributed control, where devices react to locally measurable quantities and according to a common predefined relationship or equation. The following equation shows that how the reference voltage of a typical converter in a DC microgrid is calculated based on its virtual resistance and its output current.

$$V_{ci}^* = V_{ni} - R_{di}I_{ci} \qquad (1)$$

where V_{ci}^* is the reference voltage for the ith converter, V_{ni} is the nominal voltage of the ith converter, R_{di} is the value of the virtual resistance (droop slope) and I_{ci} is the output current of the ith converter.

In this paper, we are modifying equation (1) so that the reference voltage will be dependent not only on the output current and the droop slope, but also the DC bus voltage and the nominal voltage of the converter. The reason behind this modification is that to enable features such as islanding, demand response, peak shaving, and redundancy in the micro-grid. Following equation shows which parameters are used for calculating the reference voltage of the system's converters.

$$V_{ci}^* = f(V_{ni}, V_{dc}, I_{ci}, R_{di}) \qquad (2)$$

where V_{dc} is the DC bus voltage.

Fig. 1(c) shows the schematic of a typical DC microgrid consisting of a PV array, two BESSs and a grid-tied converter. Same figure shows the I-V characteristics of the system's slack sources in two different cases and how the global voltage is determined by the balance of load and supply on the system. The distributed sources will share current according to the modified droop function discussed in equation(2). In the first case, Fig. 1(a), the BESSs (red and blue) will supply power only if the grid-tied converter and the PV cannot meet the demand, which happens if the voltage falls out of the dead-band. In the second case, Fig. 1(b), the grid-tied source (green) will supply power only if the two BESSs and the PV cannot meet the demand, which happens if the voltage falls out of the dead-band. In the other words, grid is a redundant backup source. In both scenarios, each slack source's outer control layer handles the energy management by the droop function, and the inner voltage control layer achieves instantaneous power balance and ensures stability. Block diagram of the individual converters of the system and their controllers including: modified droop controller, voltage and current controllers are shown in Fig. 2. It should be noted that the grid-tied converter is a voltage source inverter (VSI) in series with a bi-directional buck converter and the
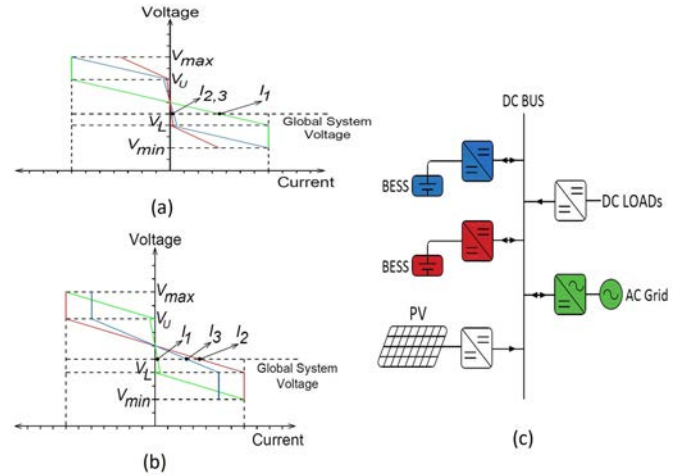

Fig. 1: (a): I-V characteristics of the slack sources in case I. (b): I-V characteristics of the slack sources in case II. (c): Schematic of a typical DC microgrid.

BESS converters assumed to be bi-directional buck converters.

III. CONTROLLER DESIGN

As it was shown in Fig. 1, the microgrid consists of a grid-tied converter, two BESS units, a PV array and DC loads. BESSs and the grid-tied converter are considered to be slack sources in this system and regulate the DC bus voltage following the modified droop-based controller discussed earlier. PV converter uses well-known perturb and observe algorithm to track the maximum power point and it can be considered as a variable current source, while loads are considered as a variable current sink. Therefore, controller design will be done for the slack sources of the system only. Table I shows the specifications of the DC microgrid which controller has been designed for.

The first step toward designing the controller is to design the inner voltage controller layer of each source with the knowledge of its topology, power rating and output filter such that it is stable under any external load fluctuations within the limits of its power rating. Secondly, the current controller is designed in such a way to be at least 10 times faster than the voltage controller so that the current controller does not affect the response time and stability of the converter. It was mentioned earlier that, the battery converters of the system are bi-directional buck converters and we also assume that the first stage of the grid-tied converter, VSI, is fast enough so that the internal DC bus of the inverter (the input voltage of the second stage) is always fixed at 1.3kV. With these assumptions, the design of voltage controllers for all the system's slack converters, will be similar to the design of voltage controller for the buck converters. This step has been discussed in details by the authors of this paper in [1].

The second step is to design the outer control layer which handles the energy management by the droop function. The
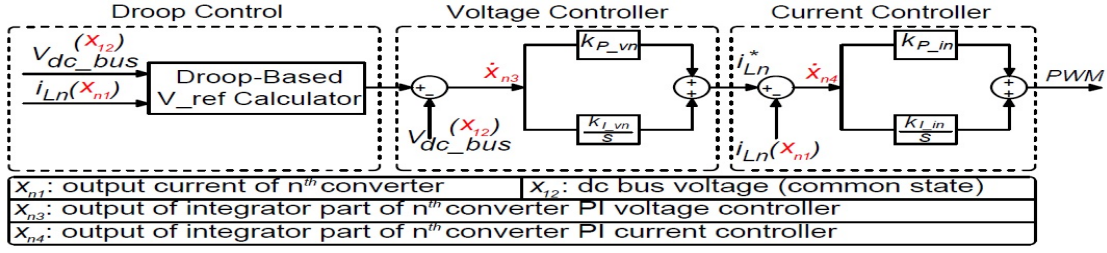
Fig. 2: Control block diagram and state definition of an individual converter in the DC microgrid.

TABLE I: Specifications of the DC Microgrid.

Component	Power Rating	Max Current	Nominal Output Voltage	Output LC Filter	Switching Frequency
Grid-Tied Converter	$60kW$	$130(A)$	$380V_{dc}$	$L = 5mH, C = 500\mu F$	$20kHz$
BESS Units (each)	$30kW$	$65(A)$	$380V_{dc}$	$L = 5mH, C = 500\mu F$	$20kHz$
PV Optimizer	$80kW$	$220(A)$	$380V_{dc}$	$L = 5mH, C = 500\mu F$	$20kHz$
Load	$50kW$	$137(A)$	$380V_{dc}$	$L = 5mH, C = 500\mu F$	$20kHz$

outer layer can be designed in number of different ways to fit the requirements of the customer. In this paper, design was done for two cases: **Case I.** where grid is the primary source responsible for regulating the DC bus voltage and BESS units are the backup to the grid. **Case II.** where BESS units are the primary sources responsible for regulating the DC bus voltage and grid is the backup to BESSs. The outcomes of these two design steps for the system shown in Fig. 1 with the specifications shown in Table I, are summarized as the following

In Both Cases:

$$
\begin{cases}
V_{min} = 365v \quad V_L = 372.5v \\
V_U = 387.5v \quad V_{max} = 395v \\
k_{P_{vG}} = 0.04 \quad k_{I_{vG}} = 2.5, k_{P_{cG}} = 1.5 \quad k_{I_{cG}} = 3.5 \\
k_{P_{vB}} = 0.25 \quad k_{I_{vB}} = 2, k_{P_{cB}} = 2.5 \quad k_{I_{cB}} = 5
\end{cases}
\tag{3}
$$

where k_P and k_I are proportional and integral gains of the PI controller. v and c subscripts stand for the voltage and current controllers respectively, while G and B stand for the grid-tied converter and BESS converter. The voltage levels are selected to keep the bus voltage withing +/-5% of the nominal voltage. Also the controller gains were calculated to ensure the stability of the system as it is discussed in the next section.

Case I: Grid is the Primary, BESSs are the Backup:

$$
\begin{cases}
V_{Grid}^* = 380 - R_{dG} * I_G \\
V_{dc} > V_U : V_{BESS}^* = 387.5 - R_{dB} * I_B \\
V_{dc} < V_L : V_{BESS}^* = 372.5 - R_{dB} * I_B \\
V_L < V_{dc} < V_U : V_{BESS}^* = 380 - 1.5 * I_B \\
R_{dG} = \frac{15}{260} \quad R_{dB} = \frac{7.5}{65}
\end{cases}
\tag{4}
$$

where V_{Grid}^* is the calculated reference voltage of the grid-tied converter, R_{dG} is the droop slope of the grid-tied converter, I_G is the output current of the grid-tied converter, V_{dc} is the DC bus voltage, V_{BESS}^* is the calculated reference voltage of the BESS converters, R_{dB} is the droop slope of the BESS converters, I_B is the output current of the BESS converters. The voltage limits as well as current ratings of the converter were used to calculate the droop coefficients.

Case II: BESSs are the Primary, Grid is the Backup:

$$
\begin{cases}
V_{BESS}^* = 380 - R_{dB} * I_B \\
V_{dc} > V_U : V_{Grid}^* = 387.5 - R_{dG} * I_G \\
V_{dc} < V_L : V_{Grid}^* = 372.5 - R_{dG} * I_G \\
V_L < V_{dc} < V_U : V_{Grid}^* = 380 - 1.5 * I_G \\
R_{dG} = \frac{7.5}{130} \quad R_{dB} = \frac{15}{130}
\end{cases}
\tag{5}
$$

It should be mentioned that in all the above expressions, currents injected to the DC bus are considered as positive and the currents drawn from the microgrid are considered negative.

IV. STABILITY ANALYSIS

In this paper, the system stability is determined by examining the eigenvalues of the state transition matrix (A matrix). The system is asymptotically stable if all the eigenvalues of the transition matrix are negative. Fig. 2 shows the control block diagram and states of an individual converter in the microgrid. From Fig. 2, the state space model of a bi-directional buck converter and its three layers of control including: current controller, voltage controller and droop control, has been derived and its A matrix can be written as the following

$$
A = \begin{bmatrix}
(\frac{-k_{P_{in}} - k_{P_{in}} k_{P_{vn}} R_{dn}}{L_n})V_{in_n} & (\frac{-\frac{1}{V_{in_n}} - k_{P_{in}} k_{P_{vn}}}{L_n})V_{in_n} \\
\frac{1}{C_n} & \frac{-1}{RC_n} \\
-R_{dn} & -1 \\
-1 - k_{P_{vn}} R_{dn} & -k_{P_{vn}} \\
(\frac{k_{P_{in}} k_{I_{vn}}}{L_n})V_{in_n} & (\frac{k_{I_{in}}}{L_n})V_{in_n} \\
0 & 0 \\
0 & 0 \\
k_{I_{vn}} & 0
\end{bmatrix}
\tag{6}
$$

where $k_{P_{in}}$ and $k_{I_{in}}$ are the PI gains of the current controller of the nth converter, respectively. $k_{P_{vn}}$ and $k_{I_{vn}}$ are the PI gains of the voltage controller of the nth converter. R_{dn} is the droop parameter of the nth converter. L_n and C_n are the output inductor and capacitor while V_{in_n} is the input voltage of the nth converter. There are different modes of operation and consequently there shall be different state space descriptions associated with each mode. Based on the previous sections, the operation modes of case I can be expressed as: **Mode I.** All the three slack sources are operating in droop mode. **Mode II.** Grid-tied converter is operating in current mode and BESSs in droop. **Mode III.** BESSs are operating in current mode and the grid-tied converter is in droop mode.

Mode I: All the three slack sources are operating in droop mode. By writing the system's equations and deriving the state space description of the system, matrix A of the system can be written as

$$
\begin{bmatrix}
a_{11} & a_{12} & a_{13} & a_{14} & 0 & 0 & 0 & 0 & 0 & 0 \\
a_{21} & a_{22} & 0 & 0 & a_{25} & 0 & 0 & a_{28} & 0 & 0 \\
-R_{d1} & -1 & 0 & 0 & 0 & 0 & 0 & 0 & 0 & 0 \\
a_{41} & a_{42} & a_{43} & 0 & 0 & 0 & 0 & 0 & 0 & 0 \\
0 & a_{52} & 0 & 0 & a_{55} & a_{56} & a_{57} & 0 & 0 & 0 \\
0 & -1 & 0 & 0 & -R_{d2} & 0 & 0 & 0 & 0 & 0 \\
0 & a_{72} & 0 & 0 & a_{75} & a_{76} & 0 & 0 & 0 & 0 \\
0 & a_{82} & 0 & 0 & 0 & 0 & 0 & a_{88} & a_{89} & a_{810} \\
0 & -1 & 0 & 0 & 0 & 0 & 0 & -R_{d3} & 0 & 0 \\
0 & a_{102} & 0 & 0 & 0 & 0 & 0 & a_{108} & a_{109} & 0
\end{bmatrix}
$$

$$(7)$$

$$a_{11} = \left(\frac{-k_{P_{i1}} - k_{P_{i1}}k_{P_{v1}}R_{d1}}{L_1}\right)V_{in1} \qquad a_{12} = \left(\frac{-\frac{1}{V_{in1}} - k_{P_{i1}}k_{P_{v1}}}{L_1}\right)V_{in1}$$

$$a_{13} = \left(\frac{k_{P_{i1}}k_{I_{v1}}}{L_1}\right)V_{in1} \qquad a_{14} = \left(\frac{k_{I_{i1}}}{L_1}\right)V_{in1}$$

$$a_{21} = \frac{1}{C_1+C_2+C_3} \qquad a_{22} = \frac{-1}{R(C_1+C_2+C_3)}$$

$$a_{25} = \frac{1}{C_1+C_2+C_3} \qquad a_{28} = \frac{1}{C_1+C_2+C_3}$$

$$a_{41} = -1 - k_{P_{v1}}R_{d1} \qquad a_{42} = -k_{P_{v1}}$$

$$a_{43} = k_{I_{v1}} \qquad a_{52} = \left(\frac{-\frac{1}{V_{in2}} - k_{P_{i2}}k_{P_{v2}}}{L_2}\right)V_{in2}$$

$$a_{55} = \left(\frac{-k_{P_{i2}} - k_{P_{i2}}k_{P_{v2}}R_{d2}}{L_2}\right)V_{in2} \qquad a_{56} = \left(\frac{k_{P_{i2}}k_{I_{v2}}}{L_2}\right)V_{in2}$$

$$a_{57} = \left(\frac{k_{I_{i2}}}{L_2}\right)V_{in2} \qquad a_{72} = -k_{P_{v2}}$$

$$a_{75} = -1 - k_{P_{v2}}R_{d2} \qquad a_{76} = k_{I_{v2}}$$

$$a_{82} = \left(\frac{-\frac{1}{V_{in3}} - k_{P_{i3}}k_{P_{v3}}}{L_3}\right)V_{in3} \qquad a_{88} = a_{11}$$

$$a_{89} = \left(\frac{k_{P_{i3}}k_{I_{v3}}}{L_3}\right)V_{in3} \qquad a_{810} = \left(\frac{k_{I_{i3}}}{L_3}\right)V_{in3}$$

$$a_{102} = -k_{P_{v3}} \qquad a_{108} = -1 - k_{P_{v3}}R_{d3}$$

$$a_{109} = k_{I_{v3}}$$

Mode II: Grid-tied converter is operating in current mode and BESSs in droop. The same procedure can be tried to find the state space description of the system in this mode. Previous state space can be applicable here considering that the droop controller as well as the voltage controller are eliminated for the grid-tied converter.

Mode III: BESSs are operating in current mode and the grid-tied converter is in droop mode. State space description for Mode I can be applicable here considering that the droop controller as well as the voltage controller are eliminated for the BESS converters.

The stable/unstable operating regions of the system for different loading conditions with respect to the controller response times are shown in Fig. 3.

Similarly, the stability of the system in case II can be examined.

V. Control-HIL Results

C-HIL realtime simulation was used to demonstrate the effectiveness and feasibility of the proposed control method. As it can be seen in Fig. 4, PV, batteries, grid and the switching converters are modeled in Typhoon HIL602 and Texas
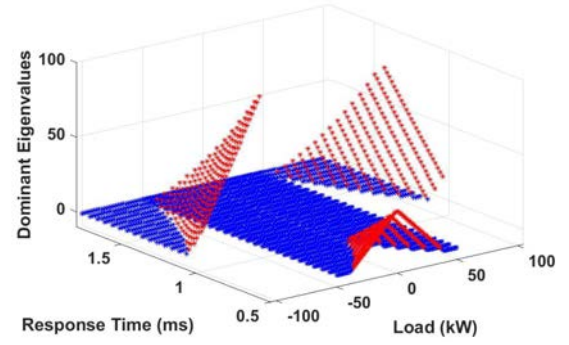

Fig. 3: Stable/unstable operating regions of case I in different loading conditions with respect to voltage controller response time.
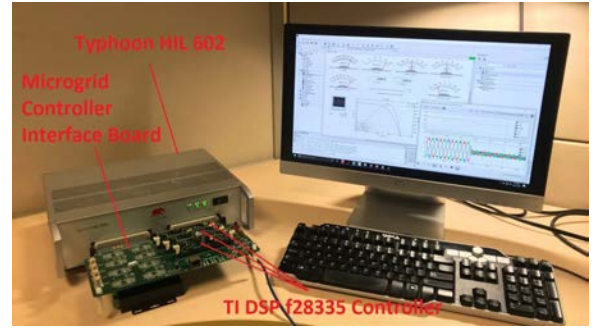

Fig. 4: C-HIL setup of the DC Microgrid.

Instruments f28335 DSPs are used to control the simulated switching converters of the systems using microgrid interface board.
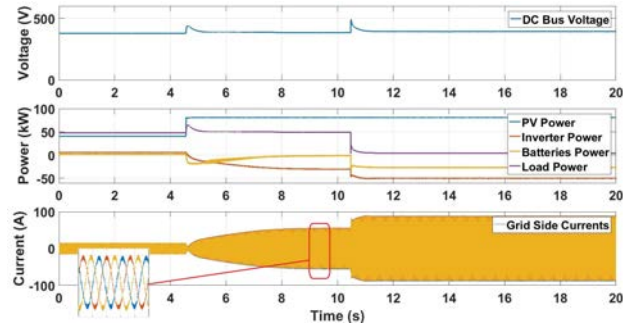
Simulation results for case I and II are summarized in Fig. 5 and 6, respectively. As it can be seen in Fig 5(a), grid is regulating the DC bus voltage between 372.5V and 387.5V while the BESSs are at standby. If the grid-tied converter cannot regulate the bus voltage due to either overgeneration or undergeneration, grid-tied converter goes to current control mode and the BESSs of the system regulate the bud voltage (Fig. 5(b)). In Fig . 5(c), grid goes out at 3.8s and the BESSs of the system start regulating the DC bus voltage and maintain the bus voltage (islanding). The results for case II is very similar to case I. However, in this case BESSs are the primary sources for regulating the bus voltage and grid is the back up. Therefore, islanding is automatically achieved.

VI. Conclusion

In this paper, we proposed a platform that is designed to enable DC microgrids by simplifying project-specific design, installation, and commissioning, allowing designers to unlock the benefits of microgrids for the customers in an economic manner. The proposed platform, utilizes a distributed control algorithm and the concept of multiple slack terminals for enabling power sharing. This structure enables microgrid ad-
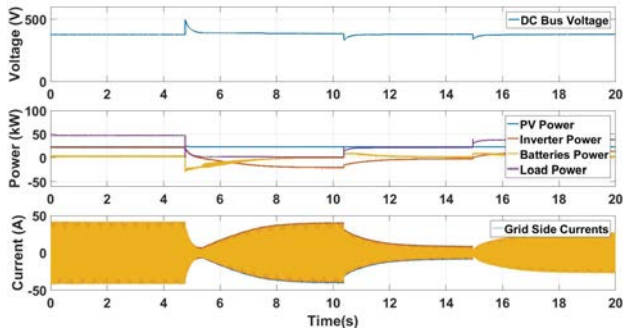
(a)

(b)
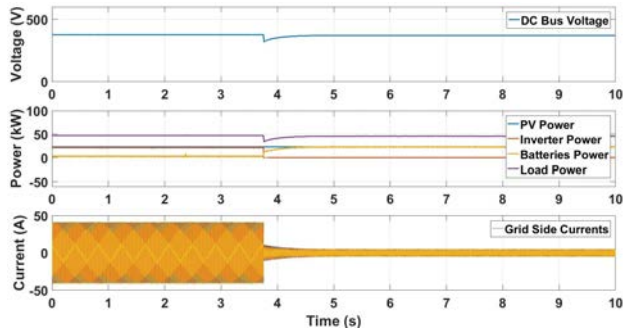
(c)

Fig. 5: Simulation results for case I: grid is the primary, BESSs are backup. (a): Grid-tied converter regulating the bus voltage and BESSs are backup. (b): BESSs helping the grid to regulate the DC bus voltage. (c): Grid connection is lost and BESSs regulate the DC bus voltage (islanding).

vantages of redundancy, simple plug-and-play, modularity and expandability. The proposed control structure was explained in details. Then, analytical stability analysis was performed to ensure the stability of the system in all the operating modes. Finally, C-HIL simulations were used for demonstrating the effectiveness of the proposed platform and control algorithm in a typical PV plus BESS grid-interactive DC microgrid.
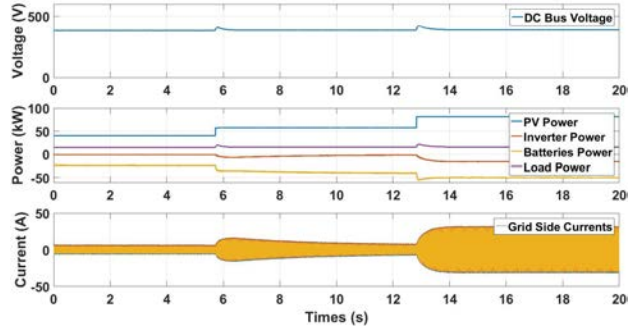
ACKNOWLEDGMENT

REFERENCES

[1] M. Mobarrez, D. Fregosi, Gh. Jalali, S. Bhattacharya, and M.A. Bahmani, "A novel control method for preventing the PV and load fluctuations in
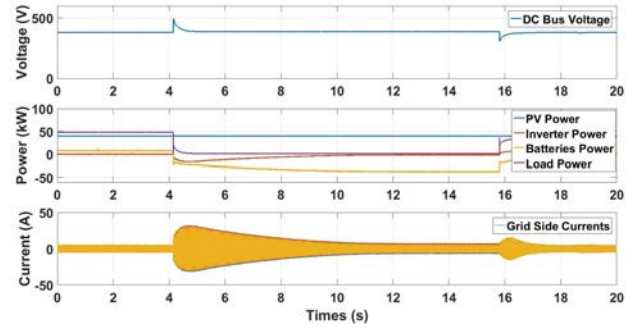
(a)

(b)

Fig. 6: Simulation results for case II: BESSs are the primary, grid is backup. (a): BESSs are regulating the DC bus voltage and grid is the backup. (b): Grid-tied converter helps BESSs to regulate the DC bus voltage.

a DC microgrid from transferring to the AC power grid", ICDCM 2017 IEEE Second International Conference on DC Microgrids, Germany, Aug 2017.

[2] M Mobarrez, S Bhattacharya, and D Fregosi, "Implementation of distributed power balancing strategy with a layer of supervision in a low-voltage DC microgrid", Applied Power Electronics Conference and Exposition (APEC), Tampa, USA, March 2017.

[3] M. Mobarrez, D. Fregosi, S. Bhattacharya, and M.A. Bahmani, "Grounding architectures for enabling ground fault ride-through capability in DC microgrids", DC Microgrids (ICDCM), 2017 IEEE Second International Conference, Germany, Jun 2017.

[4] D. Salomonsson, L. Soder, A. Sannino, "An adaptive control system for a DC microgrid for data centers", IEEE Transaction on Industry Applications, Nov. 2008.

[5] H. Kakigano, Y. Miura, T. Ise, "Distributed voltage control for DC microgrids using fuzzy control and gain-scheduling technique", IEEE Transaction on Power Electronics, Sep. 2012.

[6] C. Jin, P. Wang, J. Xiao, Y. Tang and F. H. Choo. "Implementation of Hierarchical Control in DC Microgrids". IEEE Transactions on Industrial Electronics, Aug. 2014.

[7] X. Lu, K. Sun, J. M. Guerrero, and Juan C. Vasquez, "Stability Enhancement Based on Virtual Impedance for DC Microgrids With Constant Power Loads", IEEE Transaction on Smart Grid, Nov. 2015.

[8] A. Hoke, R. B. J. Hambrick and B. Kroposki, "Maximum Photovoltaic Penetration Levels on Typical Distribution Feeders", IEEE Transaction on sustainable energy, July 2012.

[9] R. W. Erickson, D. Maksimovic, "Fundamentals of Power Electronics", MA, USA, Mar. 1997.